This thesis is dedicated

To Almighty Allah and

My

Parents

DrillBit

The Report is Generated by DrillBit Plagiarism Detection Software

Submission Information

Author Name	Salim Ali
Title	Facile Synthesis of Some Carbon and Metal Oxide-based Nanocomposites and their Applications in Biological and Environmental Sciences
Paper/Submission ID	1664053
Submitted by	nbuplg@nbu.ac.in
Submission Date	2024-04-19 11:43:30
Total Pages	189
Document type	Thesis

Result Information

Similarity **3 %**

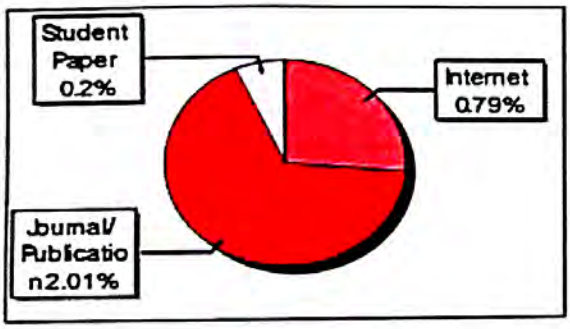

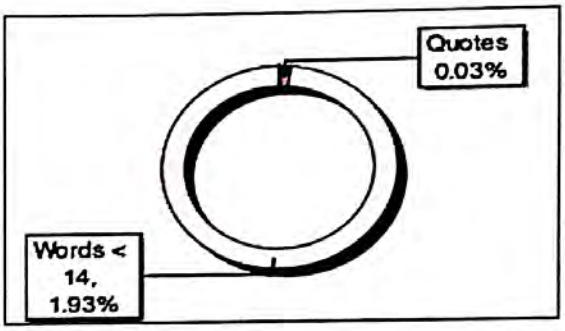

Exclude Information

Quotes	Excluded
References/Bibliography	Excluded
Sources: Less than 14 Words %	Not Excluded
Excluded Source	2 %
Excluded Phrases	Not Excluded

Database Selection

Language	English
Student Papers	Yes
Journals & publishers	Yes
Internet or Web	Yes
Institution Repository	Yes

Salim Ali

Signature of the Candidate

Mahendra Nath Roy

Signature of the Principal Supervisor

Prof. (Dr.) M. N. Roy
FRSC (London), UK
Department of Chemistry
University of North Bengal
Darjeeling-734013, India

Suranjan Sikdar

Signature of the Co-Supervisor

Dr. Suranjan Sikdar
Associate Professor of Chemistry
Ghani Khan Choudhury Institute of
Engineering & Technology, Ma

DECLARETION

I declare that the thesis entitled "**Facile Synthesis of Some Carbon and Metal Oxide-based Nanocomposites and their Applications in Biological and Environmental Sciences** "has been prepared by me under the guidance of Dr. Mahendra Nath Roy, Professor of Chemistry, University of North Bengal and Dr. Suranjan Sikdar (Co-Supervisor), Associate Professor of Chemistry, Ghani Khan Choudhury Institute of Engineering & Technology (GKCIET). No part of this thesis has formed the basis for the award of any degree or fellowship previously.

Salim Ali

SALIM ALI

Department of Chemistry

University of North Bengal

Darjeeling – 734013

West Bengal, India

Date: 20. 05. 2024

UNIVERSITY OF NORTH BENGAL

PROF (DR.) M. N. ROY
FRSC (London), UK
Senior Professor of Chemistry, NBU
Founder Vice-Chancellor of Alipurduar University, Awardee of One Time Grant from UGC, Prof. Suresh C. Ameta Award from ICS, Bronze Medal from CRSI and Shiksha Ratna, Dooars Ratna and Banga Bhushan from the Government of West Bengal

ENLIGHTMENT TO PERFECTION

Phone : 0353 2776381
Mobile: 094344 96154
Fax: +91 353 2699001
Darjeeling-734 013,
West Bengal, INDIA
May, 2024
Email:
mahendraroy2002@yahoo.co.in
/mahendraroy2018@nbu.ac.in

CERTIFICATE

I, certify that Mr. Salim Ali has prepared his thesis entitled "**Facile Synthesis of Some Carbon and Metal Oxide-based Nanocomposites and their Applications in Biological and Environmental Sciences**", for the award of **Ph.D. degree (Doctor of Philosophy)** from the University of North Bengal, under our guidance. He has carried out his work at the Department of Chemistry, University of North Bengal. The contents of this thesis, in full or in parts, have not been submitted to any other Institution or University for the award of any degree or diploma.

Mahendra Nath Roy

PROF (DR.) MAHENDRA NATH ROY,
Department of Chemistry,
University of North Bengal,
Darjeeling: 734013,
West Bengal, India

Prof. (Dr.) M. N. Roy
FRSC (London), UK
Department of Chemistry
University of North Bengal
Darjeeling-734013, India

DATE: 20-05-2024.

Ghani Khan Choudhury Institute of Engineering & Technology
गनी खान चौधरी इंजीननयररंग और प्रौद्योनगकी संस्थान
A Centrally Funded Technical Institute (CFTI) under Ministry of Education Govt of India
निक्षा मंत्रालय, भारत सरकार के तहत सीएफटीआई

Dr. Suranjan Sikdar
Associate Professor
Department of Chemistry
Narayanpur-732141, INDIA
May, 2024

Phone: 07866931531
Mobile: 09733181024
E-mail:suranium9@gmail.com/
suranjan@gkciet.ac.in

CERTIFICATE

This is to certify that Mr. Salim Ali has completed the thesis work under our guidance on the topic "**Facile Synthesis of Some Carbon and Metal Oxide-based Nanocomposites and their Applications in Biological and Environmental Sciences**", and submitted to Department of Chemistry, University of North Bengal, for the award of degree of Doctor of Philosophy in Science (Chemistry). The contents of this thesis, in full or in parts, have not been submitted to any other Institution or University for the award of any degree or diploma.

Suranjan Sikdar

Dr. Suranjan Sikdar
Associate Professor of Chemistry
Ghani Khan Choudhury Institute of
Engineering & Technology, Malda

Dr. Suranjan Sikdar,
Associate Professor,
Department of Chemistry
Ghani Khan Choudhury Institute of Engineering and Technology (GKCIET)
Narayanpur, Malda-732141,
West Bengal, India
Dt: 20/05/2024

ACKNOWLEDGEMENT

First and foremost, I would want to give thanks and appreciation to the Almighty Allah for his blessings that have enabled me to successfully complete my studies. First and foremost, I would want to convey to my esteemed supervisor and instructor, Dr. Mahendra Nath Roy, a professor in the Department of Chemistry at the University of North Bengal in Darjeeling, India, my sincere appreciation and inner sentiment. He has provided me with ongoing advice, insightful recommendations, and encouraging yet constructive criticism during my research time. I am incredibly grateful to him for his intense curiosity, drive, and unwavering support and thoughtfulness. We are grateful for his faith, encouragement, and creative freedom throughout the project. I would like to extend my sincere gratitude to my esteemed co-supervisor Dr. Suranjan Sikdar, Associate Professor in the Department of Chemistry at the Ghani Khan Choudhury Institute of Engineering & Technology (GKCIET), Malda, West Bengal, India

We are grateful for his faith, encouragement, and creative freedom throughout the project. I could not have brought my thesis to its current form without his tender care, steady direction, and priceless oversight. I would especially want to express my gratitude to our Honourable Head of the Chemistry Department at NBU, Prof. (Dr.) Bhaskar Biswas, for his constant and thorough advice and direction during the research project. I would also want to extend my sincere gratitude to the esteemed faculty members of the University of North Bengal's Department of Chemistry for their invaluable support and ongoing inspiration during my study. I am appreciative of the University of North Bengal's University Scientific Instrumentation Centre in particular for their assistance in providing me with laboratory equipment.

This acknowledges my parents' inspiration, encouragement, and unwavering collaboration in the most tasteful way. My profound thanks to my mother, Smt. SALEHA BIBI, and father, Sri HATEM ALI, for their invaluable contributions to my career development and inspiration in finishing my thesis, cannot be expressed in words. I would especially like to thank my lab partners for their invaluable support and collaboration throughout my research project. I am always conscious of how much I owe to the various books, monographs, papers, computer websites, and other sources of

knowledge that I used for my research. I would want to express my gratitude in writi to all of the references I have used for my thesis. I am grateful for the financial suppo and practical help that CSIR, with Reference No. 09/285(0092)/2019-EMR-I, has giv me to carry out my research.

Salim Ali

SALIM ALI

Department of Chemistry

University of North Bengal

Darjeeling – 734013, WB, India

Date: 20.05.2024

PREFACE

The work in the thesis entitled "**Facile Synthesis of Some Carbon and Metal oxide-based nanocomposites and their applications towards biological and Environmental Sciences"** was initiated under the supervision of Dr. Mahendra Nath Roy, Prof. of Chemistry in the Department of Chemistry, University of North Bengal. This research was become conscious within the framework of the Programme in the field of "**Nanoscience and Nano chemistry for environmental remediation and enzyme mimic properties"** and the research group of Professor Roy.

The whole is an attempt to construct the potent carbon and metal oxide nanoparticle by green and chemical method and employed these nanomaterials to environmental remediation and also applied them to colorimetric detection of some biological important molecules. Because the nanomaterials mimic bio enzyme activity and by virtue of bio enzyme activity of these nanomaterials, the colorimetric detection have been achieved in real time and cost effective way.

During the course of my research, I was privileged to participate in several meets and seminars across the country. I was highly inspired by listening and interacting with distinguished experts and scientists. I was even fortunate enough to publish the works relating the thesis in the International Journal of repute. In keeping with general practice of reporting scientific observation, due acknowledgement has been made whenever the work described was based on the findings of the other investigators. I must take the responsibility of any unintentional oversights and errors, which might have crept in spite of precautions.

I hope I will be given more challenges in my life so that the knowledge that I have earned during my work can be put into action in the future.

LIST OF TABLES

CHAPTERS	TABLES	PAGE NO.
CHAPTER-III	**Table1**: Tabular format of different enzyme-mimic kinetic parameters of $CeZrO_4$ NPs.	67
	Table S1 lattice parameters of $CeZrO_4$ NPs	68
	Table S2 lattice parameters of CeO_2 NPs	68
	Table S3 lattice parameters of ZrO_2 NPs	68
CHAPTER-IV	**Table 1:** Tabular form of K_m& V_{max} values obtained from different kinetic plots	89
	Table 2: Comparison of detection of the fluoride ion in water using different methods	89
	Table S1: Lattice parameters of $FeMnO_4$@GQD nanocomposite	90
	Table S2: Lattice parameters of $FeMnO_4$ NPs	90
	Table S3: Lattice parameters of GQD	91
CHAPTER-V	**Table 1** Tabular form of different enzyme-mimic kinetic parameters of PANI-ES, PANI-EB, GO and g-C_3N_4 NFs.	125
	Table S1: Lattice parameters and size determination table of PANI -ES nanoparticles	125
	Table S2: Lattice parameters and size determination table of PANI -EB nanoparticles	126
	Table S3: Lattice parameters and size determination table of g-C_3N_4 nanoparticles	126
	Table S4: Lattice parameters and size determination table of GO nanoparticles	127
	Table S5: Tabular format of enzyme-mimic kinetic parameters of PANI-ES compare with some other light activated oxidase mimicking nanozymes.	127
CHAPTER-VI	**Table 1:** Tabular form of different enzyme-mimic kinetic parameters of Mn_3O_4@g-C_3N_4,	170
	Table 2. Antioxidant and anti-lipid peroxidation activity of tested sample evaluated through different radical scavenging assay (data presented as Mean ± SD of triplicate determination).	170

CHAPTERS	TABLES	PAGE NO.
	Table 3: Comparison of the LOD between the proposed method and other reported method	**170**
	Table 4: Comparison of the LOD between the proposed method and other reported method	**171**
	Table S1: Lattice parameters and size determination table of 1:3 Mn_3O_4@g-C_3N_4 nanocomposite.	**171**
	Table S2: Lattice parameters and size determination table of 2:3 Mn_3O_4@g-C_3N_4 nanocomposite.	**172**
	Table S3: Lattice parameters and size determination table of 3:3 Mn_3O_4@g-C_3N_4 nanocomposite.	**172**
	Table S4: Lattice parameters and size determination table of Mn_3O_4 nanoparticles	**173**
	Table S5: Tabular format of enzyme-mimic kinetic parameters of PANI-ES compare with some other light activated oxidase mimicking nanozymes.	**173**
CHAPTER-VII	**Table 1:** Tabular form of K_m& V_{max} values obtained from different kinetic plots	**204**
	Table 2: Antioxidant activity of the CuS nanoparticles (Data presented as average ±standard deviation of triplicate determination)	**204**
	Table 3: tabular format to compare the limit of detection (LOD) between the proposed method and other reported method	**204**
	Table S1: Lattice parameters and size determination table of CuS nanoparticles	**205**
	Table S2. The Kinetics parameters Km and Vmax of TMB and H_2O_2 compared with the HRP and other nano enzymes.	**205**

LIST OF FIGURES

CHAPTERS	FIGURES	PAGE NO.
CHAPTER-I	**Fig.I.1** different kinds of carbon based materials	7
	Fig.I.2 3D structure of graphitic carbon nitride	8
	Fig.I.3 Different kinds of PANI	9
	Fig.I.4 mechanism of MB degradation by Fenton like mechanism with CeO_2	12
	Fig.I.5 Applications of nanozyme in different detection system	14
	Fig.I.6 colorimetric detection of catechol and hydroquinone by Mn3O4 nanozyme	15
	Fig.I.6 Various substrates oxidation by CuS nanozyme	18
CHAPTER-II	**Fig.II.1** Nanoparticles synthesis by sol-gel method	23
	Fig.II.2 diagram for nanoparticles synthesis by co-precipitation method.	24
	Fig.II.3 diagram for nanoparticles synthesis by green method	26
	Fig.II.4 diagram for main component of XRD.	29
	Fig.II.5 diagram for main component of scanning electron microscope.	30
	Fig.II.6 diagram for main component of transmission electron microscope.	31
	Fig.II.7 Diagram for main component of DLS.	32
	Fig.II.8 diagram for main component of FT-IR spectroscopy.	34
CHAPTER-III	**Figure 1** Schematic representation for the preparation of green synthesized $CeZrO_4$.	55
	Figure2 (a) XRD spectra of $CeZrO_4$ nanoparticles (b) and (c) SEM images of $CeZrO_4$ nanoparticles with different resolution (d) SEM image of CeO_2 nanoparticle (e) SEM image of ZrO_2 nanoparticle and (f) Size distribution of $CeZrO_4$ nanoparticles.	56
	Figure 3 *(a)* EDAX spectrum of $CeZrO_4$(b) Elemental mappings of Cerium, Zirconium and Oxygen atoms (c) FTIR spectra of CeO_2, ZrO_2 and $CeZrO_4$ nanoparticles(d) Hydrodynamic particle size distribution of $CeZrO_4$ nanoparticles	56
	Figure 4.UV–vis spectral monitoring of the peroxidase-like activity of $CeZrO_4$ compared to model indicators including (a) TMB, and (c) dopamine. (b) Peroxidase-like activity of $CeZrO_4$	57

CHAPTERS	FIGURES	PAGE NO.
	against different time interval (d) pH-dependent peroxidase-like activity of $CeZrO_4$ at wavelength of 650 nm	
	Figure 5. Steady-state kinetic analysis of $CeZrO_4$ as peroxidase mimetic. (a) Curve of velocity against the TMB concentration in condition of 10 mM H_2O_2. (c) Curve of velocity against the H2O2 concentration in conditions of 0.3 mM TMB. (B, d) Double-reciprocal plots of (a, c), respectively. Condition: 25 $\mu g \cdot mL^{-1}$ $CeZrO_4$ in acetate buffer (pH 5.0) at room temperature. Graphical representation of peroxidase mimicking activity of $CeZrO_4$ vs TMB (e)	**58**
	Figure 6. UV–vis spectral monitoring of the Oxidase-like activity of $CeZrO_4$ compared to model indicators including (a) TMB, and (c) dopamine (b) Oxidase-like activity of $CeZrO_4$ against different time interval (d) pH-dependent Oxidase-like activity of $CeZrO_4$ at wavelength of 650 nm	**59**
	Figure 7. Steady-state kinetic analysis of $CeZrO_4$ as oxidase mimetic. (a) Curve of velocity against the TMB concentration in Condition: 25 $\mu g \cdot mL^{-1}$ $CeZrO_4$ in acetate buffer (pH 5.0) at room temperature. (b) Double-reciprocal plots of (a) Graphical representation of oxidase mimicking activity of $CeZrO_4$ vs TMB (c)	**60**
	Figure 8 (a) UV–vis spectral monitoring of Degradation of MB by the $CeZrO_4$mediated Fenton-like reaction(b)Impact of time on MB degradation by the $CeZrO_4$ nanoparticles-mediated Fenton-like reaction(c)Degradation % by different synthesized nanomaterials (d) Influence of scavengers on the MB degradation by the $CeZrO_4$-driven Fenton-like reaction	**61**
	Figure 9. Study the anticancer potential of CeO_2, ZrO_2, and $CeZrO_4$ nanoparticles through MTT assay: (a)-(b) HEK-293 cell line (Human Embryonic Kidney normal cell line) was treated with different concentration of CeO_2, ZrO_2, and $CeZrO_2$ as given in methods. The bar diagrams show percentage cell viability and (c) ACHN cell line (Human Embryonic Kidney cancerous cell line) was treated with different concentration of CeO_2, ZrO_2, and $CeZrO_4$ as given in methods. The bar diagrams show percentage cell toxicity.	**62**
	Figure S1 XRD peak profile diagram of CeO_2 and ZrO_2 nanoparticles	**63**

CHAPTERS	FIGURES	PAGE NO.
	Figure S2 Hydrodynamic particle size distribution of $CeZrO_4$ nanoparticles	63
	Figure S3 Hydrodynamic particle size distribution of $CeZrO_4$ nanoparticles	64
	Figure S4. UV-vis spectra of peroxidase-like activity of $CeZrO_4$ nanoparticles (a) Substrate TMB vs NPs (b) Substrate H_2O_2 vs NPs	64
	Figure S5. UV-vis spectra of oxidase-like activity of $CeZrO_4$ nanoparticles Substrate TMB vs NPs	65
	Figure S6 UV-vis spectra of different scavengers on the MB degradation by the $CeZrO_4$ driven Fenton-like reaction	65
	Figure S7 $CeZrO_4$ NPs-based Nonenzymatic cell viability effect: live cell concentration was monitored from the OD of MTT at 570 nm against (a)HEK cell line (b) ACHN cell line.	66
	Figure S8. Shows IC50 values of ACHN cell line.	
CHAPTER-IV	**Figure1:** (a) Systematic illustration of $FeMnO_4$@GQD nanocomposites synthesis. (b) EDAX spectrum of $FeMnO_4$@GQD (c) hydration particle size of $FeMnO_4$@GQD nanocomposite (d) XRD spectra of $FeMnO_4$@GQD nanocomposite and $FeMnO_4$ NPs. (e) FT-IR spectrum of $FeMnO_4$ NPs, GQD and $FeMnO_4$@GQD nanocomposites	81
	Figure 2: SEM images of (a) $FeMnO_4$ NPs (b) GQD (c) $FeMnO_4$@GQD nanocomposite (high resolution) (d) $FeMnO_4$@GQD nanocomposite (low-resolution) and elemental mappings of (e) GQD (red color: carbon; green color: oxygen) (f) $FeMnO_4$ NPs (red color: Manganese; green color: Iron; blue color: oxygen) and (g) $FeMnO_4$@GQD nanocomposite (red color: carbon; green color: Manganese; blue color: Iron; white: oxygen)	82
	Figure 3: (a) Systematic illustration of oxidase activity Oxidase-like activity of $FeMnO_4$@GQD nanocomposite; (b) UV-vis spectral monitoring of the Oxidase-like activity of $FeMnO_4$@GQD nanocomposite compared to model indicators, TMB (c) UV-vis spectra for oxidase-like activity of $FeMnO_4$@GQD nanocomposite against different time (d) UV-vis spectra for oxidase-like activity (at wavelength 652 nm) of $FeMnO_4$@GQD nanocomposite with variation of p^H values (e) Temperature dependent oxidase activity at wavelength 652 nm.	83

CHAPTERS	FIGURES	PAGE NO.
	Figure 4: Oxidase-like activity of $FeMnO_4$@GQD nanocomposite against the substrates TMB: different kinetic plots for (a) Michele's Menten (b) Line weaver Burk (c) Hanes-Woolf (d) Eadie-Hofstee (e) The oxidase activity on four months duration (f) Different strategies to display the existence of ROS in the $FeMnO_4$@GQD nanocomposite system, NaN_3 as the $^1O_2$ scavenger, PBQ as $O_2^{\bullet-}$ scavenger, IPA as the •OH scavenger, AA as the •OH scavenger.	84
	Figure 5: (a) Graphical representation showed the oxidase inhibition in the presence of Fluoride ions. Systematic detection system illustration: (b) UV−vis absorption spectra of formation of blue-colored oxidase product (the detection system) in the presence of different concentrations of F^- ions (c) Linear relationship between the absorbance of oxidase product at 652 nm (A_{652} nm) vs. F^- ions concentrations. Digital photograph of oxidase product with varying F^- ions concentrations inset in Figure (c). (d) Calibration curve for F^- ions detection. (e) Comparison of the absorbance at 652 nm in the presence of potentially interfering substances% of inhibition of oxidase activity in F^- ions.	85
	Figure S1: XRD spectra of GQD	86
	Figure S2: EDAX spectrum of (a) $FeMnO_4$ NPs and (b) GQD	86
	Figure S3: Particle size distribution (bar diagram) from SEM of (a) GQDs (b) $FeMnO_4$ NPs and (c) $FeMnO_4$@GQD nanocomposite	87
	Figure S4: UV-visible spectra of oxidase blue product with varying temperature	87
	Figure S5: UV-visible spectra of oxidase blue product at different substrate TMB concentrations	88
	Figure S6: UV-visible spectra of oxidase blue product produced by catalyst in varying month intervals.	88
	Figure S7: UV-visible spectra of oxidase system with different scavengers IPA, AA, NaN_3 and PBQ	88
CHAPTERS-V	**Figure 1** (A) Systematic illustration of Acid polymerization synthesis of PANI-ES and PANI-EB (B) Digital photograph of synthesized PANI NFs (blue colored-PANI-EB and Green colored PANI-ES in DMSO) (C) XRD spectra of PANI-ES NFs (top) PANI-EB	111

CHAPTERS	FIGURES	PAGE NO.
	NFs (middle) and g-C_3N_4 NFs(bottom) (D) EDAX spectrum of PANI-ES NFs.	
	Figure 2 (A) ^{1}HNMR spectra of PANI-ES in DMSO **(B)** FT-IR spectra of PANI-ES and PANI-EB	**112**
	Figure 3 (A) UV -visible spectra of synthesized PANI in its emeraldine base (EB) and salt (ES) forms **(B)** systematic diagram are presented the energy diagram for PANI-EB and PANI-ES.	**112**
	Figure 4 (A–B) Representative SEM images of PANI-ES (Emeraldine salt) in different magnification (A) 1 µ m and (B) 2 µm **(C-D)** Represent the SEM images of PANI-EB (Emeraldine base) in different magnification **(C)** 1 µ m and **(D)** 2 µm **(E–F)** Representative SEM images of g-C_3N_4 in different magnification **(E)** 1 µ m and **(F)** 5 µm **(G-H)** Represent the SEM images of GO in different magnification **(G)** 1 µ m and **(H)** 2 µm **(I-J)** EDAX mapping of PANI-ES **(I)** and PANI-EB **(J)** (red-C, blue-N, green-S). **(K-L)** EDAX mapping of g-C3N4 **(K)** and GO **(L)** (red-C, blue-N, green-Oxygen)	**113**
	Figure 5 (A) graphical illustration of Oxidase-like activities of PANI NFs in catalyzing the oxidation of TMB and OPD (B) Comparison the Absorbance of TMBox with various catalyst GO, PANI-ES PANIEB, and g-C_3N_4 after sunlight irradiation and before sunlight irradiation and their corresponding digital photograph **(C)** Time dependent UV–vis absorbance of the 2.5 mg/different catalyzed oxidation of 0.480 mM **(D)** TMB and 1 mM **(G)** OPD. Time dependent UV–vis absorption spectra of **(E)** TMB, **(F)** OPD catalyzed by PANI-ES	**114**
	Figure 6 (A) pH-dependent nonzymatic activity of PANI-ES NFs. Comparison of the oxidase-like activities of PANI-ES NFs at different pH **(B)** Michaelis–Menten kinetics for the oxidation of Varying concentration (20 to 800)of TMB catalyzed by 2.5 mg/mL PANI-ES, PANI-EB, GO and g-C3N4 at room temperature and pH-5 **(C)** Double reciprocal Line weaver Burk plot with same conditions **(D)** graphical abstract for light induced ROS generation by PANI-ES **(E)** Absorbance of the PANI-ES-TMB system in the presence of different scavengers. For isopropanol, NaN3, 4-benzoquinone and Ascorbic acid **(F)** Systematic pathway to generate specific ROS in	**115**

CHAPTERS	FIGURES	PAGE NO.
	three reaction mediums. **(G)**UV−vis absorption spectra of PANI-ES-TMB system in the presence of tryptophan.	
	Figure 7 (A) Optimized geometries for the PANI-ES-TMB composite at B3LYP-D3/6-31+G (d) level of theory. Gary, white and blue color represents carbon, hydrogen and nitrogen atoms respectively. Bond lengths are in angstrom unit **(B)** Plots of reduced density gradient (RDG) for PANI-ES-TMB composite **(C)** Electrostatic potential maps for PANI-ES-TMB composite.	**116**
	Figure 8 (A) Antimicrobial activity of PANI-ES, (i) PANI-EB, (ii) GO (iii) and g-C_3N_4 against *B subtilis* (Concentration of the sample applied a=250 µg/ml, b=100 µg/ml, c=50 µg/ml) **(B)** Antimicrobial activity of PANI-ES, (i) PANI-EB(ii),GO (iii) and g-C_3N_4 against *Bmegaterium*(Concentration of the sample applied a=250 µg/ml, b=100 µg/ml, c=50 µg/ml) **(C)** Antimicrobial activity of PANI-ES, (i) PANI-EB, (ii) GO (iii) and g-C_3N_4 against *S aureus* (Concentration of the sample applied a=250 µg/ml, b=100 µg/ml, c=50 µg/ml) **(D)** Zone of inhibition of Gram positive bacteria (i) *B.subtilis* (ii) *B. megaterium* (iii) *S. aures* treatment by different nanozymes.	**117**
	Figure 9 (A) Antimicrobial activity of PANI-ES (i), PANI-EB(ii),GO (iii) and g-C_3N_4 against *S typhimurium* (Concentration of the sample applied a=250 µg/ml, b=100 µg/ml, c=50 µg/ml) **(B)** Antimicrobial activity of PANI-ES (i), PANI-EB(ii),GO (iii) and g-C_3N_4 against *E coli* (Concentration of the sample applied a=250 µg/ml, b=100 µg/ml, c=50 µg/ml) **(C)** Zone of inhibition of Gram negative bacteria (i) *S.typhimurium* (ii) *E. coli* treatment by different nanozymes.	**118**
	Figure S1: molecular structure of catalyst (A) PANI-ES, (B) PANI-EB	**119**
	Figure S2: XRD spectra of GO	**119**
	Figure S3. ^{1}HNMR spectra of PANI-EB in DMSO	**119**
	Figure S4. (A) The band gap of PANI-ES (B) FTIR spectra of PANI-ES	**120**
	Figure S5 Size calculation histogram of different nanoparticles (A) PANI-ES, (B) GO, (C) PANI-EB, (D) g-C3N4	**120**
	Figure S6 (A−B) Representative TEM images of PANI-ES	**121**

CHAPTERS	FIGURES	PAGE NO.
	(Emeraldine salt) in different magnification (A) 200 nm and (B) 100 nm (C) Size of PANI-ES from TEM image.	
	Figure S7: UV-visible plots of TMBox catalysed by different catalyst at pH-5, catalytic dose 2.5 mg/mL and 480 µM TMB concentration (A) Under solar light irradiation (B) Without solar light irradiation.	**121**
	Figure S8: UV-visible plots of (A) OPD catalysed by catalyst and without catalyst (B) TMB catalysed by catalyst and without catalyst.	**121**
	Figure S9: UV-visible plots of (A) TMB catalysed by PANI-ES in the presence of varying interfering agents. (B) Bar diagram of absorbance of TMB catalysed by PANI-ES in the presence of varying interfering agents.	**122**
	Figure S10 Systematic illustrated the formation of TMBox and TMBdi	**122**
	Figure S11 Hans Woolf kinetics for the oxidation of varying concentration (20 to 800) of TMB catalysed by 2.5 mg/mL PANI-ES (A), GO (C), g-C3N4 (E) and PANI-EB (G) at room temperature and pH-5. Double reciprocal Eadie plot in same conditions of PANI-ES (B), GO (D) g-C3N4 (F) PANI-EB (G)	**123**
	Figure S12. (A) UV-visible spectra of TMBox formation in different environment N_2 atmosphere and O_2 saturated atmosphere treated. (B) Fluorescence intensities of hydroxy Coumarin in presence of PANI-ES, Conversion of 7- hydroxy Coumarin (C). Time-dependent UV−vis absorption spectra of nitro blue tetrazolium (NBT) treated with PANI-ES in slight basic medium with 2.5 mg/mL catalytic dose, NBT transform to formazan in presence of superoxide radical (showing below) coumarin from Coumarin in presence of hydroxyl radical (showing below)).(D) $^1O_2$-mediated generation of different product from tryptophan (singlet oxygen involvement)	**124**
CHAPTER-VI	**Fig. 1. (A)** Schematic diagram of Mn_3O_4 @g-C_3N_4 preparation. **(B)** The diagrammatic representation of Mn_3O_4 @g-C_3N_4 catalyzed variety of chromogenic reaction (DA, TMB, and CA) and antioxidant enzyme mimics.	**153**
	Fig. 2 (A) XRD of Mn_3O_4@g-C_3N_4 and Mn_3O_4 (1-1:3 Mn_3O_4@g-	**154**

CHAPTERS	FIGURES	PAGE NO.
	C_3N_4, 2-1:2 Mn_3O_4@g-C_3N_4, 3- 3:3 Mn_3O_4@g-C_3N_4) **(B)** FT-IR spectrum of Mn_3O_4@g-C_3N_4 and Mn_3O_4 (1-1:3 Mn_3O_4@g-C_3N_4, 2-1:2 Mn_3O_4@g-C_3N_4, 3- 3:3 Mn_3O_4@g-C_3N_4).Representative FE-SEM images of 3:3 Mn_3O_4@g-C_3N_4 in different magnification **(C)** 500 nm and **(D)** 1 µm **(G)** Represent the SEM images of Mn_3O_4 in magnification 1 µ m. **(H)** Representative SEM images of g-C_3N_4 in magnification 1 µ m. EDAX mapping of 3:3 Mn_3O_4@g-C_3N_4 **(E,F,I,J)**.	
	Fig. 3 TEM image **(A)** Mn_3O_4 **(E)** g-C_3N_4 **(F)** 3:3 Mn_3O_4@g-C_3N_4, magnification 500 nm **(G)** 3:3 Mn_3O_4@g-C_3N_4, magnification.HR-TEM images **(B)** Mn_3O_4 **(J)** 3:3 Mn_3O_4@g-C_3N_4. SEAD pattern **(C)** Mn_3O_4 **(I)** 3:3 Mn_3O_4@g-C_3N_4 **(D)** Size of Mn_3O_4 (blue) and 3:3 Mn_3O_4@g-C_3N_4 (pink) calculated by image-j software. EDAX pattern of 3:3 Mn_3O_4@g-C_3N_4 **(K)** table of % of element by weight of 3:3 Mn_3O_4@g-C_3N_4 **(H)**	**155**
	Fig. 4 (A) diagrammatical representation of Oxidase and peroxidase-mimic activities catalyzed by Mn_3O_4@g-C_3N_4 Vs TMB as a substrate **(B)** Time dependent UV-visible spectra of TMB ox catalyzed by 3:3 Mn_3O_4@g-C_3N_4, at p^H-5, TMB (400 µ M) at room temperature. **(C)** Time dependent absorbance Vs TMB catalyzed by g-C_3N_4 and (3:3, 3:2, 3:1) - Mn_3O_4@g-C_3N_4 at p^H-5, TMB (400 µ M) at room temperature. **(D)** effect of p^H on oxidase mimic activity... **(E)** Michaelis–Menten kinetics of varying concentration (50 to 350 µ M) of TMB catalyzed by 0.5 mg/mL Mn_3O_4@g-C_3N_4 at p^H-5, at room temperature **(F)** Double reciprocal Line weaver Burk plot with same conditions oxidase activity **(G)** Radar plot showed absorbance of the 3:3-Mn_3O_4@g-C_3N_4-TMB system in the presence of different scavengers. Isopropanol, NaN3, 4-benzoquinone and Ascorbic acid **(H)** Bar graph showed the absorbance changed in the presence of different concentration tryptophan.	**156**
	Fig. 5(A) Comparison of oxidase and peroxidase mimic catalyzed by different catalyst (1-Mn_3O_4, 2-g-C_3N_4 3-3:3-Mn_3O_4@g-C_3N_4, 4-2:3-Mn_3O_4@g-C_3N_4 5-1:3-Mn_3O_4@g-C_3N_4). (**B**) Time dependent UV-visible spectra of TMB ox catalyzed by 2:3-Mn_3O_4@g-C_3N_4, at p^H-4, H_2O_2 (10 m M), TMB (400 µ M) at room temperature. **(C)**	**157**

CHAPTERS	FIGURES	PAGE NO.
	Effect of p^H on peroxidase mimic activity catalyzed by 2:3-Mn_3O_4@g-C_3N_4, at H_2O_2 (10 m M), TMB (400 µ M) at room temperature. **(D)** Michaelis–Menten kinetics of varying concentration (1 to 16 m M) of H_2O_2 catalyzed by 0.5 mg/mL Mn_3O_4@g-C_3N_4 at p^H-4, at room temperature	
	Fig. 6. (A) Systematic representation of CAT and SOD mimic activity **(B)** digital Picture of CAT mimic activity catalyzed by (3:3, 2:3, 1:3)- Mn_3O_4@g-C_3N_4 at p^H-9, TMB at room temperature **(1-**1:3 Mn_3O_4@g-C_3N_4, 2-2:3 Mn_3O_4@g-C_3N_4, 3-3:3Mn_3O_4@g-C_3N_4) **(C)** UV–vis spectra of CAT-like activity for H_2O_2 (5 m M), catalyzed by all catalyst (1mg/ml), at p^H-9, room temperature**. (G)** p^H effect on catalase mimic activity by 3:3-Mn_3O_4@g-C_3N_4 (1mg/ml), at room temperature **(D)** Steady state kinetics, Michalis –Menten plot **(E)** Line weaver Burk plot as a catalase mimic H_2O_2 (2-10 m M),catalyzed by 3:3 (1mg/ml), at p^H-9, room temperature.	**158**
	Fig.7 (A) UV-visible absorption spectra of O_2 ·−-NBT system in the presence of all catalyst (1 mg/mL) p^H – 7.4, room temperature **(B)** UV-visible absorption spectra of O_2 ·−-NBT system by varying concentration of 3:3 Mn_3O_4@g-C_3N_4 (0.0-2.00 mg/mL), p^H -7.4 room temperature **(C)** p^H effect on catalase mimic activity by 3:3-Mn_3O_4@g-C_3N_4 (1mg/ml), at room temperature **(D)**The relationship between inhibition of NBT reduction with concentration of 3:3-Mn_3O_4@g-C_3N_4 (0.0-2.00 mg/mL)), p^H -7.4 and logarithm of 3:3 Mn_3O_4@g-C_3N_4 concentrations linear fit relation. **(E)** Schematic diagram of self-made device for extraction of cigarette smoke. **(F)** Bar diagram of $O^{2\cdot-}$ scavenging ability of 3:3-Mn_3O_4@g-C_3N_4 NPs in different brand cigarette smoke extract.	**159**
	Fig 8: (A) Systematic diagram of Mn_3O_4@g-C_3N_4 catalyzes the dismutation of O_2•− into H_2O_2, and the decomposition of H_2O_2 into O_2 and water and elimination of toxic ·OH subsequently **(B)** Absorption spectra of SA after reaction with Fe^{2+}/H_2O_2, in the absence and presence of Mn_3O_4 NPs. SA alone, and SA reacted with Fe^{2+} or H_2O_2 were used as control. Radar plot depicting the inhibition percentage of studied samples against DPPH radical in different (tested) concentrations **(C)** ABTS radical in different (tested) concentrations **(D)** superoxide radical in different	**160**

CHAPTERS	FIGURES	PAGE NO.
	(tested) concentrations **(E)** lipid peroxidation in different (tested) concentrations **(F).**	
	Fig. 9. Colorimetric detection of CA and H_2Q **(A)** UV-visible spectra of TMB-3:3 Mn_3O_4@g-C_3N_4, system in the presence of varying concentrations of CA (0−320 µ M), 0.4 mM- TMB, 0.5 mg·mL^{-1} 3:3 Mn_3O_4@g-C_3N_4 composites, pH 5.0, room temperature **(B)** Absorbance at 652 nm of colorimetric detection with different CA concentrations. The linear fit of the detection Vs the concentration of CA inset the Fig. (B). **(C)** UV- visible spectra and the corresponding photographs after adding different interference solutions. 0.4 mM -TMB, 0.5 mg·mL^{-1} 3:3 Mn_3O_4@g-C_3N_4 composites, pH 5.0, room temperature. **(D)** UV-visible spectra of TMB-3:3 Mn_3O_4@g-C_3N_4, system in the presence of varying concentrations of H_2Q (0−320 µ M), 0.4 mM-TMB, 0.5 mg·mL^{-1} 3:3 Mn_3O_4@g-C_3N_4composites, pH 5.0, room temperature **(E)** Absorbance at 652 nm of colorimetric detection with different H_2Q concentrations. The linear fit of the detection Vs the concentration of H_2Q inset the **Fig. (E).**	**161**
	Fig.10 Systematic diagram of CA and H_2Q discrimination by colour **(A).** UV-visible spectra of TMB-Mn_3O_4@g-C_3N_4/CA system started after 1 hours **(B).**UV-visible spectra of CA oxidation catalyzed by 0.5 mg/mL Mn_3O_4@g-C_3N_4 at p^H-8, at room temperature **(C).** Michaelis−Menten kinetics CA oxidation catalysed by 0.5 mg/mL Mn_3O_4@g-C_3N_4 at p^H-8, at room temperature **(D)**. Double reciprocal Line weaver Burk plot with same conditions oxidase activity **(E).** Time dependent UV-visible spectra of DA oxidation catalyzed by 3:3 Mn_3O_4@g-C_3N_4, at p^H-8, at room temperature **(F).** Time dependent UV-visible spectra of H_2Q oxidation catalyzed by 3:3 Mn_3O_4@g-C_3N_4, at p^H-8, at room temperature **(G).**	**162**
	Figure S1: (A) XRD spectra of Urea. (B) XRD of g-C_3N_4	**163**
	Figure S2: FT-IR spectra of g-C_3N_4	**163**
	Fig. S3: SEM images of 1:3Mn_3O_4@ g-C_3N_4 (A). SEM images of 2:3Mn_3O_4@ g-C_3N_4 (B).	**164**
	Fig.S4 UV-visible spectra of TMBox catalyzed by 1:3 Mn_3O_4@g-C_3N_4, at p^H-5, TMB (400 µ M) at room temperature (A) UV-visible spectra of TMBox catalyzed by 2:3 Mn_3O_4@g-C_3N_4, at p^H-5, TMB (400 µ M) at room temperature (B)	**164**

CHAPTERS	FIGURES	PAGE NO.
	Fig.S5 Digital picture of TMB oxidation catalyzed by 3:3 Mn_3O_4@g-C_3N_4, at p^H-5, TMB (400 µ M) at room temperature at different pH	**164**
	Fig. S6 Hans Woolf kinetics for the oxidation of varying concentration (50 µ M to 350 µ M) of TMB catalyzed by 0.5 mg/mL 3:3 Mn_3O_4@g-C_3N_4, at p^H-5, TMB at room temperature **(A)**. 0.5 mg/mL 2:3 Mn_3O_4@g-C_3N_4, at p^H-5, TMB at room temperature **(C)**. 0.5 mg/mL 1:3 Mn_3O_4@g-C_3N_4, at p^H-5, TMB at room temperature **(E)**. Eadie kinetics for the oxidation of varying concentration (50 to 350) of TMB catalyzed by 0.5 mg/mL 3:3 Mn_3O_4@g-C_3N_4, at p^H-5, TMB at room temperature **(B)**. 0.5 mg/mL 2:3 Mn_3O_4@g-C_3N_4, at p^H-5, TMB at room temperature **(D).** 0.5 mg/mL 1:3 Mn_3O_4@g-C_3N_4, at p^H-5, TMB at room temperature **(F).**	**165**
	Fig.S7 (A) Digital picture of TMB oxidation catalyzed by 3:3 Mn_3O_4@g-C_3N_4, at p^H-5, TMB (400 µ M) at room temperature in N_2 atmosphere (left) and natural atmosphere (right). UV-visible spectra of TMBox catalyzed by 3:3 Mn_3O_4@g-C_3N_4, at p^H-5, TMB (400 µ M) at room temperature in N2 atmosphere and natural atmosphere **(B).**	**166**
	Fig.S8 Absorbance Vs H_2O_2 concentration TMB catalyzed by Mn_3O_4 at p^H-5, TMB (400 µ M) at room temperature **(A)** Absorbance of TMB oxidation catalyzed by 0.5 mg/mL g-C_3N_4 at p^H-5, at room temperature **(B)**.	**166**
	Fig. S9 Digital picture of TMB oxidation catalyzed by 3:3 Mn_3O_4@g-C_3N_4, and H_2O_2 at p^H-5, TMB (400 µ M) at room temperature **(A).** Line weaver Burk kinetics for the oxidation of varying concentration (2 to 16 mM) of H_2O_2 catalyzed by 0.5 mg/mL 2:3 Mn_3O_4@g-C_3N_4, at p^H-5, TMB at room temperature **(B)**.	**167**
	Fig.S10 Fluorescence intensities of hydroxyl terepthalic acid (TAOH) in presence H_2O_2 catalyzed by 3:3 Mn_3O_4@g-C_3N_4, 2:3 Mn_3O_4@g-C_3N_4, 1:3 Mn_3O_4@g-C_3N_4 Mn_3O_4 and g-C_3N_4 at p^H-5, at room temperature	**167**
	Fig.S11 UV-visible spectra of H_2O_2 in different concentration **(A).** UV-visible spectra of decomposition of different concentration H_2O_2 catalyzed by 3:3 Mn_3O_4@g-C_3N_4, at p^H-9, at room temperature **(B)**	**168**

CHAPTERS	FIGURES	PAGE NO.
	Fig.S12 Digital picture of SOD mimic activity catalyzed by1.control 2. Catalyzed by g-C_3N_4 3. Catalyzed by 1:3 Mn_3O_4@g-C_3N_4, 4. Catalyzed by 2:3 Mn_3O_4@g-C_3N_4, 5. catalyzed by 3:3 Mn_3O_4@g-C_3N_4, at p^H-7.4, at room temperature	**168**
	Fig.S13 Digital picture of TMB oxidation catalyzed by 3:3 Mn_3O_4@g-C_3N_4, at p^H-5, TMB (400 µ M) at room temperature with control (initial) NO_3^- (middle) and ClO_4^- (last) ions **(A).** UV-visible spectra of TMBox catalyzed by 3:3 Mn_3O_4@g-C_3N_4, at p^H-5, TMB (400 µ M) at room temperature with NO_3^- and ClO_4^- ions **(B).**	**169**
	Fig.S14 (A) Digital picture of CA oxidation catalyzed by 3:3 Mn_3O_4@g-C_3N_4, at p^H-8, at room temperature UV-visible spectra of different concentration CA oxidation catalyzed by 3:3 Mn_3O_4@g-C_3N_4, at p^H-8, at room temperature.	**169**
CHAPTER-VII	**Figure 1.** (a) Schematic diagram of the fabrication procedure for CuS NPs, (b) XRD pattern of CuS NPs, (c) size determination bar graph CuS NPs (d), (e) SEM images of CuS NPs in different resolution and (f) elemental mapping distribution of CuS NPs (green-Sulphur atom, blue- Cu atom)	**191**
	Figure. 2 TEM image **(A)** CuS NPs magnification 50 nm **(B)** SEAD pattern CuS NPs **(C)** Size distribution histogram of CuS NPs calculated by image-j software. **(D)** HR-TEM image of CuS NPs	**192**
	Figure 3. (a) Diagrammatic representation of peroxidase and Oxidase like activity of CuS NPs with TMB and Dopamine. Time dependent absorbance by different systems TMB (380 µM+ H_2O_2 (20 mM) and CuS NPs (0.5 mg/mL) (b) vs different condition in same time (c) vs time. Time dependent absorbance by different systems Dopamine (0.5 mM) + H_2O_2 (20 mM) and CuS NPs (0.5 mg/mL) (d) vs different condition in same time. Absorbance of TMB (380 µM) + CuS NPs (0.5 $mgml^{-1}$) + H_2O_2 (20 mM) system in different p^H (e). Absorbance of TMB (380 µM) + CuS NPs (0.5$mgml^{-1}$) + H_2O_2 (20 mM) system in presence of different scavengers (f).	**193**
	Figure 4 Steady state kinetic analysis of CuS NPs as peroxidase mimetic: (a) Curve of velocity against the TMB concentration in condition of 20 mM H_2O_2, room T, p^H 5. (c) Curve of velocity against the H_2O_2 concentration in conditions of 380 µ M TMB, room T, p^H 5. (b, d) Double-reciprocal plots of (a, c) respectively	**194**
	Figure 5. Fluorescence spectra of TA+ CuS NPs+H_2O_2	**194**

CHAPTERS	FIGURES	PAGE NO.
	Figure 6: NBT react with superoxide to form formazan (a) SOD-mimic activity. (b) UV-visible spectra of O_2 ·−-NBT system contains CuS NPs (0.5 mg/mL) at pH – 7.4, (c) UV-visible spectra of O_2 ·−-NBT system with different concentration of CuS NPs (0.05-1.00 mg/mL), at pH -7.4. (d) The inhibition of NBT reduction vary with the concentration of CuS (0.05-1.00 mg/mL), at pH -7.4 and in situ the relation of linear fit of inhibition % and logarithm of CuS concentrations. (e) Graphical picture of self-made device for cigarette smoke extraction. (f) Bar diagram of O_2 ·− scavenging ability of CuS NPs in different brand cigarette smoke extract.	195
	Figure 7: (a) diagrammatical representation of Peroxidase and SOD mimic activities catalyzed by CuS NPs **(b)** Comparative effect of synthesized CuS nanoparticles against different types of free radical depicted the % of activity.	196
	Figure 8 (a). UV-visible spectra peroxidase system (TMB 480 µM+ H_2O_2 20 mM and CuS NPs (0.5 mg/mL) under varying concentration of Epinephrine (EP) (b) ΔAbs. vs Concentration (EP) plot, (c) linear fit Plots of absorbance versus (EP) concentration. (d) Bar diagram of Abs, of peroxidase system (TMB 480 µM+ H_2O_2 20 mM and CuS NPs (0.5 mg/mL) in the presence of different interfering agent.	197
	FigS1: (A) Zeta potential plot of CuS Nanoparticles. **(B)** Zeta potential plot of CuS NPs+ BSA.	198
	Fig S2. Peroxidase like activity of CuS NPs vs Dopamine. UV–vis absorption spectra of the CuS NPs + H_2O_2 and Dopamine	199
	Fig S3. Peroxidase like activity of CuS NPs vs p^H. UV–vis absorption spectra of the CuS NPs 0.5 mg/mL + 380 µM + H_2O_2 20 mM TMB in different p^H	199
	FigS4 Systematic illustration of the formation of TMBox and TMBdi	200
	Fig S5. Peroxidase like activity of CuS NPs vs temperature. **(A)**.UV–vis absorption spectra of the CuS NPs 0.5 mg/mL + 380 µM + H_2O_2 20 mM TMB in different Temperature.**(B).** Radar plot of the CuS NPs 0.5 mg/mL + 380 µM + H_2O_2 20 mM TMB in	200

CHAPTERS	FIGURES	PAGE NO.
	different Temperature	
	Fig. S7. Peroxidase like activity of Varying TMB and H_2O_2 concentrations. UV–vis absorption spectra of the CuS NPs 0.5 mg/mL+ H_2O_2 20 mM and Varying TMB concentrations. (a) UV–vis absorption spectra of the CuS NPs 0.5 mg/mL + 380 µM TMB and Varying H_2O_2 concentrations.	**201**
	Fig. S8: Hans Woolf kinetics for the oxidation of (a) Varying concentration (60 to 720 µM) of TMB catalysed by CuS NPs 0.5 mg/mL+ H_2O_2 20 mM (c) Varying concentration (10 to 150 mM) of H_2O_2. Double reciprocal Eadie plot of (b) Varying concentration (60 to 720 µM) of TMB catalysed by CuS NPs 0.5 mg/mL+ H_2O_2 20 mM (d) Varying concentration (10 to 150 mM) of H_2O_2 + CuS NPs 0.5 mg/mL + 380 µM TMB.	**201**
	Fig. S9 UV–vis absorption spectra of MB with CuS (0.5mg/mL)+30 mM H_2O_2 (a) UV–vis absorption spectra of MB with CuS (0.5mg/mL)+30 mM H_2O_2 with different Scavengers.	**202**

ABBREVIATIONS

AA	Ascorbic acid
µm	Micrometre
Å	Angstrom
G	Glucose
GL	Glycine
Al	Alanine
Cm	Centimetre
F	Folic acid
EP	Epinephrine
eV	Electron Volt
Fig.	Figure
U	Uric Acid
G	Gram
Try	Tryptophan
DA	Dopamine
FTIR	Fourier Transform Infrared spectroscopy
K	Kelvin
M	Molar
m	Meter/Molality
mg	Milligram
min	Minute
mL	Millilitre
µM	Micromolar
µL	Microlitre
^{0}C	Degree Celsius
rpm	Revolutions Per Minute
SEM	Scanning Electron Microscopy
TGA	Thermogravimetric Analysis
DSC	Differential Scanning Calorimetry
UV-vis	Ultraviolet-visible
NMR	Nuclear Magnetic Resonance
XRD	X-Ray Diffraction

List of Appendix

APPENDIX A List of Publications

APPENDIX B List of Seminars/Conferences Attended

APENDIX-A
LIST OF PUBLICATIONS

1. **Salim Ali,** Suranjan Sikdar, Shatarupa Basak, Modhusudan Mondal, Kangkan Mallick, Md Salman Haydar, Shibaji Ghosh, Debadrita Roy , Shibaji Ghosh , Sanjay Sahu , Paramita Paul , Mahendra Nath Roy, Label-Free Detection of Epinephrine Using Flower-like Biomimetic CuS Antioxidant Nanozymes.

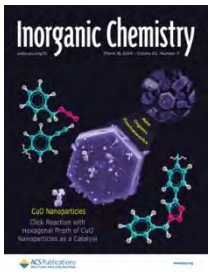

2023, Inorganic Chemistry, ACS

(Included in the Thesis)

2. **Salim Ali,** Suranjan Sikdar, Shatarupa Basak, Modhusudan Mondal, Kangkan Mallick, Md Salman Haydar, Shibaji Ghosh, Mahendra Nath Roy, Assemble multi-enzyme mimic tandem Mn3O4@ g-C3N4 for augment ROS elimination and label free detection.**,**

2023, Chemical Engineering Journal

(Included in the Thesis)

3. **Salim Ali,** Suranjan Sikdar, Shatarupa Basak, Debadrita Roy , Dipayan Das, Md Salman Haydar, Narendra Nath Ghosh , Kanak Roy, Palash Mandal Mahendra Nath Roy Intrinsic Light-Activated Oxidase Mimicking Activity of Conductive Polyaniline Nanofibers: A Class of Metal-Free Nanozyme.

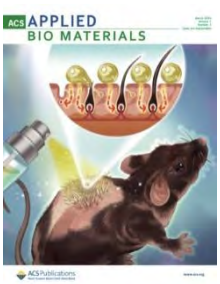

2022, ACS Applied Bio Materials

(Included in the Thesis)

4. **Salim Ali** , Suranjan Sikdar , Shatarupa Basak , Debasmita Das , Debadrita Roy , Md Salman Haydar , Vikas Kumar Dakua , Prakriti Adhikary , Palash Mandal , Mahendra Nath Roy Synthesis of β-Cyclodextrin Grafted Rhombohedral-CuO Antioxidant Nanozyme for Detection of Dopamine and Hexavalent Chromium through off-on Strategy of Peroxidase Mimicking activity.

2022, Microchemical Journal

(not Included in the Thesis)

5. **Salim Ali** , Suranjan Sikdar , Shatarupa Basak , Md Salman Haydar , Vikas Kumar Dakua , Prakriti Adhikary , Palash Mandal , Mahendra Nath Roy, β-Cyclodextrin-Stabilized Biosynthesis Nanozyme for Dual Enzyme Mimicking and Fenton Reaction with a High Potential Anticancer Agent.

2022, ACS Omega

(Included in the Thesis)

6. **Salim Ali**, Dr. Suranjan Sikdar, Shatarupa Basak, Debadrita Roy, Dr. Vikas K Dakua, Dr. Prakriti Adhikary, Prof. Mahendra N. Roy, High Visual Colorimetric Determination of F- Ions by Exploiting the Inhibition of Oxidase Mimicking Activity of FeMnO4@GQD Nanocomposite,

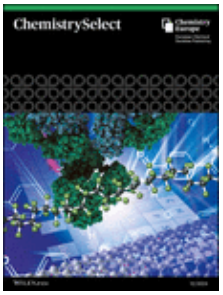

2022, Chemistry Select, **(Included in the Thesis)**

7. **Salim Ali,** Shatarupa Basak, Suranjan Sikdar, MahendraNath Roy, Synergetic effects of green synthesized CeO2 nanorod-like catalyst for degradation of organic pollutants to reduce water pollution,

2021, Environmental Nanotechnology Monitoring and Management,

(not Included in the Thesis)

8. Shatarupa Basak, Suranjan Sikdar, **Salim Ali,** Modhusudan Mondal, Debadrita Roy, Vikas Kumar Dakua and Mahendra Nath Roy, Synthesis and characterization of Mo $_x$ Fe $_{1-x}$ O nanocomposites for the ultra-fast degradation of methylene blue via a Fenton-like process: a green approach

2022, New Journal of Chemistry **(not Included in the Thesis)**

9. Debasmita Das, **Salim Ali,** Biplab Rajbanshi, Samapika Ray, Sanjoy Barman, Divya Chouhan, Md Salman Haydar, Palash Mandal, Kanak Roy, Vikas Kumar Dakua, and Mahendra Nath RoyInvestigation of Synthesis of Biogenic Hematite Nanocubes for environmental Assessment and its innovative Applications associated with Antibacterial, Antifungal, and Antioxidant activity

2022, ACS Omega

(not Included in the Thesis)

10. Shatarupa Basak, **Salim Ali,** Modhusudan Mondal, Debadrita Roy, Ankita Dutta, Anoop Kumar, Suranjan Sikdar, Mahendra Nath RoyGreen Synthesis and Characterization of Heterostructure MnO-FeO Nanocomposites to Study the Effect on Oxidase Enzyme Mimicking, HSA Binding Interaction and Cytotoxicity,

2021, Chemical Physics Letter

(not Included in the Thesis)

11. Suranjan Sikdar, Afroja Banu, **Salim Ali,** Subhodeep Barman, Pankaj Lal Kalar, Dr. Rahul Das Micro-structural Analysis and Photocatalytic Properties of Green Synthesized t-ZrO_2 Nanoparticles,

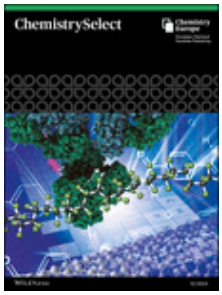

2022, Chemistry select, **(not Included in the Thesis)**

12. Modhusudan Mondal,Shatarupa Basak, **Salim Ali,** Debadrita Roy, Subhadeep Saha, Narendra Nath Mahendra Nath Exploring inclusion complex of an anti-cancer drug (6-MP) with b-cyclodextrin and its binding with CT- DNA for innovative applications in anti-bacterial activity and photostability optimized by computational study

2022, RSC Advanced

(not Included in the Thesis)

13. Shatarupa Basak, **Salim Ali**, Debasmita Das, Suranjan Sikdar, Mahendra Nath Roy Synthesis, Characterization and Visible Light Induced Photo-Degradation of Acid Orange II Dye in Aqueous Medium using a Novel Synthesized Al2MoZnO7 Nanocomposite,

2020, Journal of Advanced Chemical Sciences,

(not Included in the Thesis)

14. Biswajit Ghosh, Niloy Roy, Debadrita Roy, Saikat Mandal, **Salim Ali**, Pranish Bomzan, Kanak Roy, Mahendra Nath Roy, An Extensive Investigation on Supramolecular Assembly of a Drug (MEP) with βCD for Innovative Applications

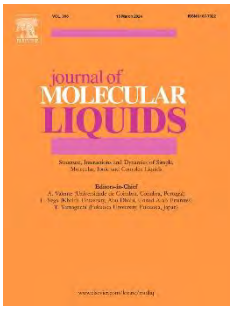

, 2020, journal of molecular liquid

(not Included in the Thesis)

15. Modhusudan Mondal, Shatarupa Basak, Debadrita Roy, Subhadeep Saha, Biswajit Ghosh, **Salim Ali,** Narendra Nath Ghosh, Ankita Dutta, Anoop Kumar, Mahendra Nath Roy. Cyclic oligosaccharides as controlled release complexes with food additives (TZ) for reducing hazardous effects,

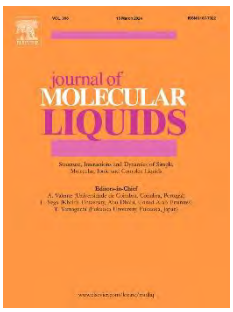

2020, journal of molecular liquid

(not Included in the Thesis)

APPENDIX-B

LIST OF SEMINARS/CONFERENCES ATTENDED

1. National Web-Based Conference on "Environmental Determinism, Diverse Pollutions, Sources, and Controlling Management Through Sciences and Humanities" Organised by: Alipurduar University, 22nd and 23rd March, 2021. ***(Presented a paper)***

2. International Seminar on "Frontiers in Chemistry **2021**" Organised by: Department of Chemistry, University of North Bengal & CRSI North Bengal Local Chapter. ***(Presented a poster)***

3. The National Science Day, ''Global Science for Global Wellbeing' ***(Presented a poster)***